

RESEARCH ARTICLE

Islet is a key determinant of ascidian palp morphogenesis

Eileen Wagner¹, Alberto Stolfi², Yoon Gi Choi³ and Mike Levine^{1,*}

ABSTRACT

The anterior-most ectoderm of ascidian larvae contains the adhesive papillae, or palps, which play an important role in triggering the metamorphosis of swimming tadpoles. In *Ciona intestinalis*, the palps consist of three conical protrusions within a field of thickened epithelium that form late in embryogenesis, as tailbuds mature into larvae. The palp protrusions express the LIM-homeodomain transcription factor *Islet*. Protrusion occurs through differential cell elongation, probably mediated by *Islet*, as we find that ectopic expression of *Islet* is sufficient to promote cell lengthening. FGF signaling is required for both *Islet* expression and palp morphogenesis. Importantly, we show that *Islet* expression can rescue the palp-deficient phenotype that results from inhibition of FGF signaling. We conclude that *Islet* is a key regulatory factor governing morphogenesis of the palps. It is conceivable that *Islet* is also essential for the cellular morphogenesis of placode-derived sensory neurons in vertebrates.

KEY WORDS: *Islet*, LIM domain, Ascidian, Cell shape, Palps, Placode

INTRODUCTION

Ascidians belong to the Subphylum Tunicata, and, as such, represent the sister group to the vertebrates (Delsuc et al., 2006). The experimental tractability, genomic simplicity and phylogenetic placement of ascidians allow for analysis of evolutionary origins of key vertebrate innovations, such as the second heart field and cranial placodes (Mazet et al., 2005; Stolfi et al., 2010). The vertebrate placodes are transient, focal ectodermal thickenings that arise within a horseshoe-shaped territory flanking the anterior neural plate in developing embryos. They contribute to the paired sense organs of the head as well as sensory components of cranial ganglia (Schlosser, 2010; Streit, 2008), and are believed to have been an important factor in the radiation of vertebrates (Gans and Northcutt, 1983).

The adhesive papillae, or palps, of ascidian tadpoles are a specialized region of the anterior-most ectoderm that might represent an ancestral placode. They develop from an ectodermal thickening that arises at the anterior border of the neural plate, and give rise to peripheral neurons, the axons of which project into the sensory vesicle (simple brain) (Imai and Meinertzhagen, 2007; Takamura, 1998). The cell lineage that gives rise to the palps expresses a variety of transcription factors that function in vertebrate placode development, including *eyes-absent*, *DMRT*, *FoxG*, *Emx*, *COE*, *Dlx-c* and *Islet* (Caracciolo et al., 2000; Giuliano et al., 1998;

Mazet et al., 2005; Park and Saint-Jeannet, 2010; Tassy et al., 2010; Tresser et al., 2010). Papillae of various ascidian species are reported to consist of three cell types: secretory cells and two types of neurons (Dolcemascolo et al., 2009; Imai and Meinertzhagen, 2007). The palp neurons have been proposed to function in both chemo- and mechanosensation.

The palps perform two crucial and related functions for the tadpole. First, they secrete the adhesive substance(s) and thus serve as the attachment site when larvae settle upon a solid substrate. Second, this attachment event serves as the trigger for the complex, multistep process of metamorphosis, in which the motile larval body plan is reorganized into a sessile, filter-feeding form (Nakayama-Ishimura et al., 2009; Sasakura et al., 2012). Arguably, the choice of settlement site is the single most important event in the life history of ascidians, as it will directly impact on opportunities for feeding and reproduction, which for sessile animals are limited by the immediate environment. There is evidence that ascidian larvae discriminate among possible settlement sites, responding to both biotic and abiotic factors (Groppelli et al., 2003; Pennati et al., 2009; Svane and Young, 1989; Torrence and Cloney, 1983), and it seems probable that neural activity in the palps controls both settlement and metamorphosis.

Despite the importance of the palps for ascidian biology, their development and physiology remained poorly defined. To better understand palp development, we performed expression profiling on sorted palp cells and identified *Emx* as enriched in the palp lineage. At the late tailbud stage, *Emx* is expressed in a striking ring-shaped pattern, and this discovery prompted our investigation of *Islet*, which is expressed in the center of the *Emx* rings. We show that expression of *Islet* correlates with protrusion of the palps in maturing tadpoles and that protrusion occurs by differential cell lengthening within the placode epithelium. Additionally, we find that *Islet* misexpression throughout the palp ectoderm promotes the protrusion of a single, large palp. Furthermore, ectopic expression of *Islet* in non-placodal ectoderm is sufficient to promote cell elongation. The fibroblast growth factor-MAP kinase (FGF-MAPK) signaling cascade is required for *Islet* expression in the palp primordia of tailbud stage embryos. Whereas perturbation of FGF signaling in the anterior neural tissue inhibits development of the palps, expression of *Islet* can rescue this defect. Thus, we conclude that *Islet* is a key regulatory factor governing morphogenesis of the palps.

RESULTS

***Emx*, *Buttonhead* and *Islet* mark the presumptive palps**

In an effort to identify new genes involved in development of the palps, we performed expression profiling on isolated cells from the palp lineage. The mouse cell surface antigens CD4 and CD8 were expressed in various tissues of the embryo, which allows enrichment of specific cell populations with antibody-coupled magnetic beads. CD4 was expressed in the palp lineage using the *FoxC* enhancer. CD8 was expressed with the *ZicL* enhancer and used for negative selection of the central nervous system (CNS), muscles and mesenchyme. Negative selection was important because the *FoxC* enhancer sometimes drives low-level ectopic expression in parts of the CNS.

¹Center for Integrative Genomics, Division of Genetics, Genomics, and Development, Department of Molecular and Cell Biology, University of California-Berkeley, Berkeley, CA 94720, USA. ²New York University, Center for Developmental Genetics, Department of Biology, 1009 Silver Center, 100 Washington Square East, New York, NY 10003-6688, USA. ³Functional Genomics Laboratory, Department of Molecular and Cell Biology, University of California-Berkeley, 255 Life Sciences Addition #3200, Berkeley, CA 94720-3200, USA.

*Author for correspondence (mlevine@berkeley.edu)

Received 1 April 2014; Accepted 4 June 2014

RNA was isolated from the sorted palp cells and from the CD8-expressing cell population and processed for hybridization to Affymetrix GeneChip microarray (GEO number GSE57920; see Methods in the supplementary material for details of the cell sorting and expression profiling protocols).

We found that the homeodomain transcription factor *Emx* (empty spiracles, *ems* in *Drosophila*) was enriched in the palp lineage of neurula stage embryos (5.1-fold enrichment, $P=4.4 \times 10^{-4}$). Interestingly, a previously published *in situ* pattern for *Emx* showed it to be expressed in an arc-shaped pattern in the anterior neural plate (Imai et al., 2004). This pattern appears similar to that of another homeodomain transcription factor, *Six1/2* (Imai et al., 2004), so we performed double *in situ* hybridization (ISH) to characterize these patterns in more detail. We found that *Emx* and *Six1/2* are expressed in the anterior-most region of the neural plate in sequential arc-shaped stripes (Fig. 1A–A'''). *Emx* is mainly expressed more anteriorly, but is also detected in some of the adjacent posterior *Six1/2*-expressing cells. In tailbud stage embryos, we found that *Emx* is expressed in a ring-shaped pattern corresponding to the three presumptive palps and also in the epidermis overlying the sensory vesicle (Fig. 1B,B').

We next compared the ring-shaped *Emx* pattern to those of two known palp markers, *Buttonhead* (*Btd*) and *Islet*. *Btd* (also known as *Sp8* or *ZF220*) is expressed in the palp lineage at the early tailbud stage, downstream of *FoxC*, the earliest marker of the palp lineage (Ikeda et al., 2013; Imai et al., 2004, 2006). In late tailbud embryos, *Btd* appears to be co-expressed with *Emx* in the rings, and also occurs in the intervening anterior-most ectoderm, but is specifically excluded from the center of the rings (Fig. 1C–C'''). The LIM-homeodomain (LIM-HD) transcription factor *Islet* marks a number of vertebrate placodes and, in *Ciona*, is expressed in three discrete foci marking the presumptive palps (Giuliano et al., 1998; Park and

Saint-Jeannet, 2010). We found that *Islet* is expressed in the center of the *Emx* rings, and might also be co-expressed with *Emx* in the rings, but not in the intervening ectoderm (Fig. 1D–D''').

Islet expression correlates with palp protrusion

Upon closer inspection, we found that *Islet* expression correlates with protrusion of the palps during maturation of tailbud embryos into larvae. *Islet* transcripts are detected in the three presumptive palps of late tailbud embryos (Fig. 2A). A close-up view of an individual palp reveals that the *Islet* transcript is specifically detected in the protrusion, as revealed by Hoechst counterstaining (Fig. 2B–C'). We have isolated an enhancer for *Islet* located in the first intron that drives reporter (mCherry) expression in the palps, and also sometimes in the notochord and the pigmented otolith, which are also normal sites of *Islet* expression (Fig. 2D). The anterior ectoderm of the late tailbud adopts a thickened, columnar epithelial shape, characteristic of ectodermal placodes. The means by which the palps protrude from the anterior surface of the embryo appears to be a simple cell shape change within this thickened epithelium (Manni et al., 2004). The cells expressing the *Islet* reporter are elongated in comparison to the neighboring, non-expressing cells (Fig. 2E,E'). In mature larvae, the tips of the palps bear fine, fingerlike projections, as revealed by phalloidin staining (Fig. 2F,G). Of note, we find that these projections derive from the *Islet*⁺ cells in the palps (Fig. 2G').

We then measured the correlation between protrusion of the palps and expression of the *Islet* reporter in late tailbud embryos. Tailbuds that develop three detectable palp protrusions express the *Islet* reporter to the greatest extent (Fig. 2H). Sometimes the orientation of the embryo on the slide makes it difficult to clearly discern all three palps, and sometimes, even under control conditions, the palps do not develop normally. The trend is clear, however: as the number of detectable palp protrusions decreases, so does expression of the

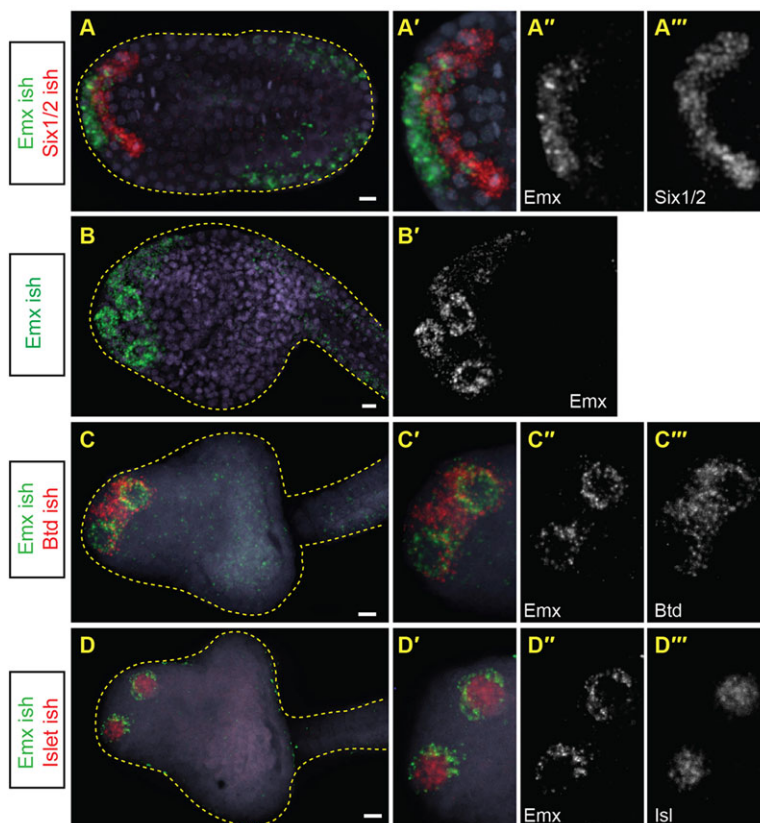


Fig. 1. *Emx*, *Btd* and *Islet* mark the presumptive palps.

(A) Double ISH of late neurula stage embryo. *Emx* transcripts detected with fluorescein-labeled probe (green) are expressed in the anterior-most neural plate, as well as the posterior (tail) ectoderm. *Six1/2* transcripts detected with DIG-labeled probe (red) are expressed in anterior neural plate posterior to the *Emx* expression domain. (B) Late tailbud stage embryo hybridized with *Emx* probe (DIG-labeled). *Emx* is expressed in three rings that delimit the presumptive palp protrusions, and also weakly in the dorsoanterior ectoderm. (C) Double ISH, late tailbud embryo. *Emx* transcript is detected with fluorescein-labeled probe (green); two of three presumptive palps are shown. *Btd* transcripts are detected with DIG-labeled probe (red) and occur with *Emx* in the rings and also in ectoderm between the rings. (D) Double ISH of late tailbud embryo. *Islet* probe (DIG-labeled, red) is detected in spots corresponding to the presumptive palp protrusions and is flanked by rings of *Emx* expression (fluorescein-labeled, green). (A',B',C',D') Close-up views of corresponding panels, focused on palp region. Nuclei are stained with Hoechst 33342. (A'',A''',B',C'',C''',D'',D''') *In situ* signal of respective single probes shown for clarity. Scale bars: 10 μ m.

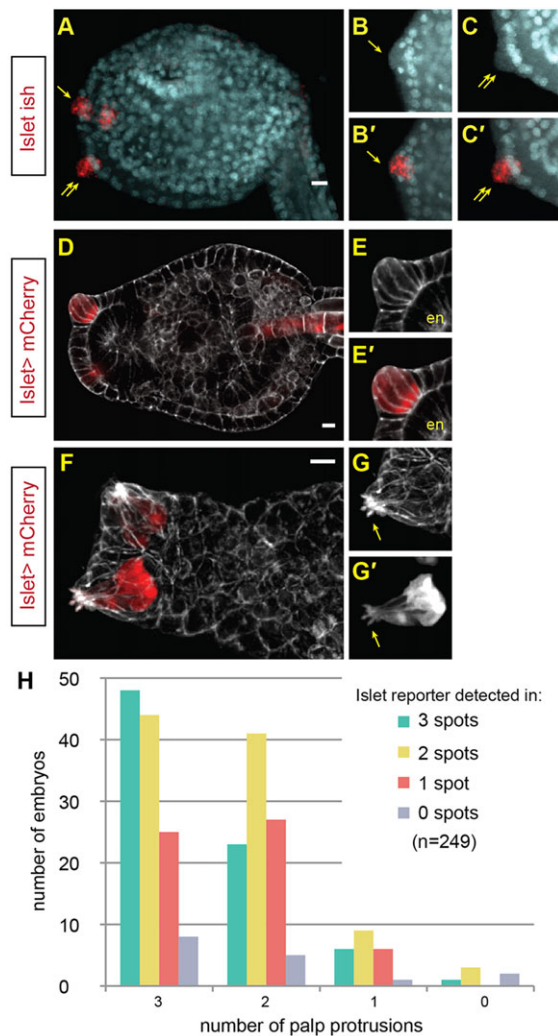


Fig. 2. *Islet* expression correlates with palp protrusion. (A) *In situ* hybridization reveals *Islet* transcript in the three presumptive palps at late tailbud stage. Image shown is a confocal z-projection of 15 slices. Two of the three presumptive palps, indicated by single and double arrows, are shown in magnified view in panels B–C'. (B–C') Confocal z-projections of two slices focused on an individual palp protrusion. (B,C) Hoechst 33342 counterstaining allows visualization of protruding palp. (B',C') Same images as in B and C, but with *Islet in situ* signal overlaid. (D–E') *Islet>mCherry* reporter is expressed in the palps of late tail bud embryo. Image shown is a confocal z-projection of four slices focused on one palp. Phalloidin staining reveals cell cortices. Cells expressing *Islet* reporter are elongated in comparison to neighboring non-expressing cells. (F–G') *Islet>mCherry* reporter expression in a mature larva, with phalloidin counterstaining. G shows phalloidin only; arrow indicates digitiform protrusions at tips of palps. G' shows *Islet* reporter only, revealing that the digitiform protrusions (arrow) derive from the *Islet*⁺ cells. (H) Correlation between protrusion of palps and *Islet* expression. Late tailbud embryos were electroporated with *Islet>mCherry* reporter plasmid and stained with phalloidin (as in D). The number of palp protrusions and the number of spots of *Islet* expression were documented. Data shown are summed from three biological replicates, 249 embryos in total were scored. en, endoderm. Scale bars: 10 μ m.

Islet reporter, and we rarely detect *Islet* reporter activation in the absence of the protrusions.

***Emx* can repress *Islet* and palp protrusion**

We next examined the regulatory relationship between *Emx* and *Islet* in palp development. To perturb gene expression in the palps, we used an enhancer for *FoxC*, which is expressed in the palp

lineage at the 112-cell stage, the time at which palps become specified. Expression of the control transgene *FoxC>lacZ* does not alter palp morphogenesis, as visualized by *FoxC>H2B:Cherry* and *Islet>YFP-caax* (membrane-targeted YFP) reporter genes (Fig. 3A). However, upon misexpression of full-length *Emx* (*FoxC>Emx*), or a constitutive repressor form consisting of the DNA-binding domain fused to the WRPW repressor motif (*FoxC>Emx:WRPW*), loss of *Islet* reporter expression occurs in the palps (Fig. 3B,C,E). Mosaic misexpression of the *FoxC>Emx* and *FoxC>Emx:WRPW* transgenes results in corresponding losses of individual palp protrusions, whereas the unelectroporated halves develop a normal palp (Fig. 3B,C).

These results suggest that *Emx* acts as a transcriptional repressor, which is consistent with the presence of a conserved engrailed homology domain in the N-terminus (Jackman et al., 2000). Thus, it is possible that the ring-shaped pattern of *Emx* expression (Fig. 1B) in the presumptive palps functions to limit the expression of *Islet* to discrete foci, but it is currently unknown whether the endogenous *Emx* repressor regulates *Islet* *in vivo*.

***Islet* misexpression promotes protrusion of a single, large palp**

We next tested the effect of *Islet* misexpression on palp development. We hypothesized that ectopic *Islet* expression throughout the palp ectoderm might drive the protrusion of a single palp rather than three distinct entities. Indeed, we found that expression of *FoxC>Islet* led to the formation of a single, large palp (Fig. 3D, compare with Fig. 3A). We further found that embryos expressing a repressor form of *Islet*, *FoxC>Islet:WRPW*, fail to express the *Islet* reporter and to protrude palps (Fig. 3F). This suggests that *Islet* acts as a transcriptional activator, and that *Islet* target genes are required to drive protrusion of the palps.

Islet expression in the palps might be subject to autoregulatory feedback. Expression of the *Islet>YFPcaax* reporter gene is restricted to discrete foci in control embryos (Fig. 3A), but is ectopically activated throughout the palp ectoderm upon expression of the *Islet*-coding sequence using the *FoxC* enhancer (Fig. 3D). *FoxC>Islet:WRPW* not only repressed palp protrusion but also eliminated expression of the *Islet>YFP-caax* reporter gene, although expression persisted in the notochord cells, which did not express *Islet:WRPW* (Fig. 3F). Thus, a positive autoregulatory mechanism might help to ensure maintenance of *Islet* expression following onset. In zebrafish embryos, a similar autoregulatory mechanism serves to maintain *Isl2* expression in Rohon–Beard neurons and sensory neurons of the trigeminal placode (Segawa et al., 2001).

We next asked whether *Islet* misexpression could repress *Emx*, to determine whether a mechanism of mutual repression might be responsible for their complementary expression patterns in the palps. We found that expression of *FoxC>Islet* did not affect *Emx* expression in the palps (supplementary material Fig. S2). We then tested the effect of simultaneous co-expression of *Emx* and *Islet* on palp development, to determine whether *Islet* expression could overcome the repressive effect mediated by *Emx*. Indeed, a protrusive single palp forms in the presence of *FoxC>Emx* and *FoxC>Islet* (Fig. 3G), similar to that develops in the presence of *FoxC>Islet* alone. This suggests that *Islet* activity is epistatic to *Emx* in the regulation of target genes required for palp protrusion.

***Islet* promotes cell elongation**

The single large palp that forms upon *FoxC>Islet* expression appeared to have cells elongated beyond the range seen under

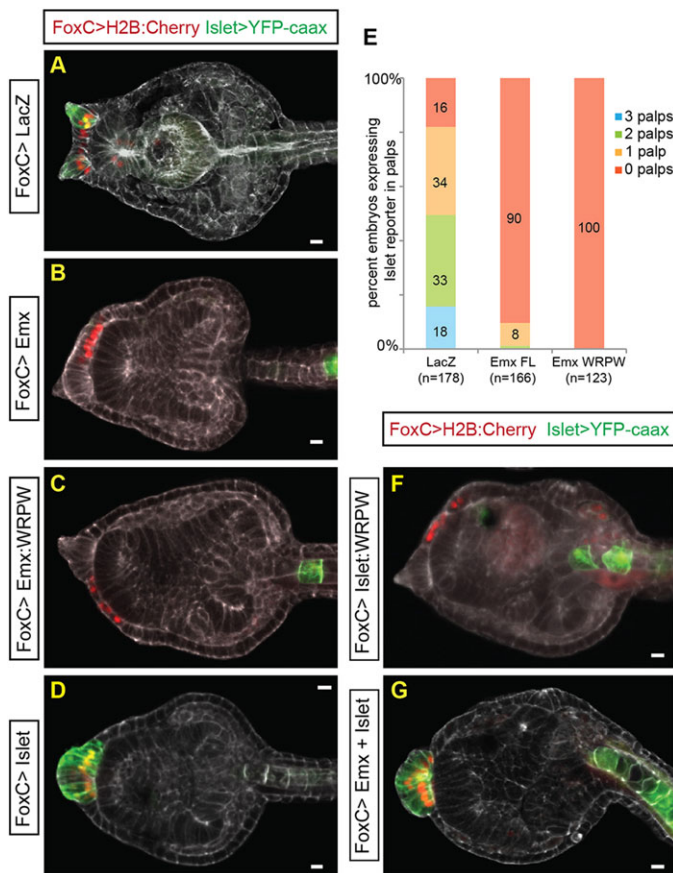


Fig. 3. *Emx* and *Islet* exert differential effects on both *Islet* expression and palp development. (A–D, F, G) Embryos were electroporated with *FoxC>H2B:Cherry* and *Islet>YFPcaax* reporter plasmids and stained with phalloidin. (A) Control embryo expressing *FoxC>lacZ* shows *Islet* reporter expression in protrusive palps. (B) Mosaic embryo shows expression of the *Islet* reporter and protrusion of the palps are repressed in the presence of full-length *Emx*, whereas protrusion occurs normally on the unelectroporated side. (C) Mosaic embryo expressing *FoxC>Emx:WRPW* (constitutive repressor) does not express *Islet* reporter in the palps and does not protrude palps on the electroporated side. (D) Expression of *FoxC>Islet* leads to a single palp protrusion and ectopic activation of *Islet* reporter. (E) Quantification of results shown in A–C. To the right (3 palps, 2 palps, etc.) is shown the number of discrete foci detected that expressed the *Islet* reporter. (F) Mosaic embryo expressing *FoxC>Islet DBD:WRPW* (constitutive repressor) shows repression of *Islet* reporter in the palps and loss of protrusion on the perturbed side. (G) Co-expression of *FoxC>Emx* and *FoxC>Islet* leads to a single, protrusive palp and ectopic activation of *Islet* reporter. Scale bars: 10 μ m.

normal conditions. The palps, however, might be biased toward cell elongation because they derive from a placode. We therefore expressed *Islet* in a region of non-placodal ectoderm to assay its effect on cell shape. An enhancer for the *FoxF* gene has been described (Beh et al., 2007), which drives expression in the trunk and tail ectoderm. We examined mosaic embryos and found that expression of *FoxF>Islet* results in trunk ectodermal cells that are elongated in comparison to cells on the unelectroporated side of the embryo (Fig. 4B–B"). By contrast, trunk ectoderm cells of mosaic embryos expressing the *FoxF>lacZ* control plasmid are of similar size (Fig. 4A–A").

To better characterize this effect, we analyzed 20 mosaic embryos, each expressing either *FoxF>lacZ* or *FoxF>Islet*, and normalized cell lengths on the perturbed side to cell lengths on the unelectroporated side. We found that cells of control embryos show little variation in size

(Fig. 4C; supplementary material Fig. S3). Expression of *FoxF>Islet*, however, reproducibly promotes cell lengthening, with effects ranging from ~1.3-fold to 2.2-fold as compared with unelectroporated cells in the same embryo (Fig. 4C; supplementary material Fig. S4). These results are highly significant, with $P=6.8 \times 10^{-8}$, according to the Wilcoxon two-sample test. We conclude that *Islet* expression is sufficient to promote cell shape changes in an ectopic context. *Islet* might thus function both as a determinant of cell identity and a regulator of cell shape (see Discussion).

FGF-MAPK signaling is required for proper *Islet* patterning

Previous work identified the FGF-MAPK signaling pathway as an important regulator of both specification and subsequent morphogenesis of the palps (Hudson et al., 2003; Wagner and Levine, 2012). Specifically, we showed that perturbation of FGF-MAPK signaling led to ectopic *FoxC* expression, but larvae that developed under these conditions failed to develop palps. A recent study revealed that, whereas *FoxC* is a marker of the palp lineage, it is not a marker of palp fate; *FoxC* expression in the palp lineage persists under conditions that inhibit palp development (Ikeda et al., 2013). Moreover, *Islet* expression is lost upon MAPK inhibition from the 8-cell stage onward, and MAPK signaling through the neurula stage is reported to be required for normal palp development (Hudson et al., 2003). We therefore examined the timing of the FGF-MAPK signaling requirement for *Islet* expression in the palps.

We expressed a dominant-negative FGF receptor (DN FGFR) in the palp lineage using the *FoxC* enhancer and found that *Islet* reporter activity in the palps was lost (Fig. 5A–C). We next used the MEK inhibitor U0126 to block MAPK signaling at later developmental time points, mid-gastrula and mid-neurula. We found that treatment at mid-gastrula stage led to loss of *Islet* transcripts in the palp region, although expression in the notochord and A10.57 motoneuron persisted (Fig. 5E, compare with control Fig. 5D; and see Discussion). Interestingly, MAPK inhibition at the mid-neurula stage led to ectopic *Islet* expression in a U-shaped pattern, appearing as though the three discrete foci seen in the wild-type condition are fused in the treated tailbuds (Fig. 5F). This result suggests that localized repressors might delimit *Islet* expression, although it is unlikely that *Emx* functions in this capacity, as its expression is unaffected by U0126 treatment (supplementary material Fig. S5). We conclude that sustained MAPK signaling is required for proper patterning of *Islet* in the presumptive palps.

Islet rescues palp development upon inhibition of FGF signaling

We next asked whether *Islet* expression could rescue the palplless phenotype that results from inhibition of FGF signaling. We previously used the *DMRT* enhancer to misexpress DN FGFR in the anterior neural plate, which gives rise to the palps and the anterior sensory vesicle (brain) of larvae. This treatment leads to ectopic *FoxC* expression, a truncated sensory vesicle and impaired palp development (Fig. 6B, compare with control larva in Fig. 6A) (Wagner and Levine, 2012). Combining the *DMRT>DN FGFR* perturbation with *FoxC>Islet*, however, led to a rescue of palp development. Cells misexpressing *Islet* become elongated, to an even greater extent than in wild-type palps (Fig. 6C, compare with Fig. 6A). This treatment leads to a larger palp than that obtained with the *FoxC>Islet* transgene (Fig. 3D), as inhibition of FGF signaling results in an increase in the number of *FoxC*-expressing cells, and a corresponding expansion in the misexpression of *Islet*.

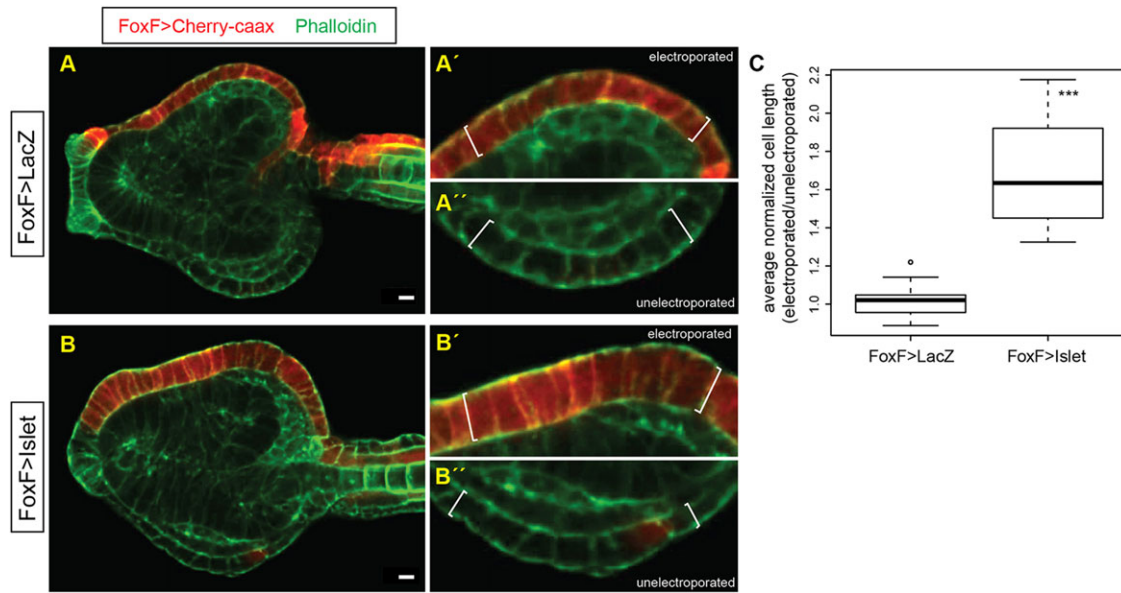


Fig. 4. *Islet* promotes cell elongation. Embryos expressing *FoxF>Cherry-caax* and *FoxF>lacZ* (A) or *FoxF>Islet* (B) were stained with phalloidin and examined by confocal microscopy. A' and A'' show close-up view of surface ectodermal cells (shown in white brackets) on electroporated and unelectroporated sides, respectively, of the *FoxF>lacZ* control. Cells on either side are of similar length. B' and B'' show magnified view of cells on the electroporated and unelectroporated sides of embryos expressing *FoxF>Islet*. Cells on electroporated side are markedly elongated in comparison to the unperturbed cells. (C) Box plot summary of cell length measurements of 20 embryos, each expressing either *FoxF>lacZ* or *FoxF>Islet*. Measurements were performed manually with ImageJ software (all images with measurements are shown in the supplementary material). Statistical significance calculated with Wilcoxon two-sample test, $P=6.8 \times 10^{-8}$. Scale bars: 10 μ m.

We then tested whether the giant palp observed in the rescue experiment bore any similarity to normally differentiated palps. One known marker of palp differentiation is β -crystallin, which is expressed in approximately two cells per palp in mature larvae (Shimeld et al., 2005). Under control conditions, we detect the β -crystallin>GFP reporter in the palps (Fig. 6D) in 73% of larvae; it is always specifically expressed in 1–2 cells per palp. Under the rescue condition, however, we detect a dramatic increase in the expression of β -crystallin>GFP reporter, with 100% of embryos showing ectopic expression (Fig. 6E,F). This suggests that β -crystallin is expressed downstream of *Islet*, as it is expressed in all cells ectopically expressing *Islet*. This also indicates that the giant palp that develops in the rescue condition bears some resemblance to a wild type. We therefore conclude that *Islet* is a key factor regulating palp morphogenesis.

A summary of palp development from specification to morphogenesis is shown in Fig. 7.

DISCUSSION

We have presented evidence that the LIM-HD transcription factor *Islet* directs the cell elongation that results in the palp protrusions of *Ciona* tadpoles. *Islet* expression in the palps occurs precisely in the regions of protrusion (Fig. 2B–C'), and we rarely observe activation of the *Islet>mCherry* reporter in the absence of protrusions (Fig. 2H). Perturbations that inhibit *Islet* expression (misexpression of either *Emx*, Fig. 3B, or *DN FGFR*, Fig. 6B) also inhibit palp development. Notably, however, co-expression of *Islet* with either *Emx* (Fig. 3G) or *DN FGFR* (Fig. 6C,E) rescues the palp-deficient phenotype observed when either *Emx* or *DN FGFR* is expressed alone. Palps that develop under the rescue condition (*DN FGFR+Islet*) express the differentiation marker β -crystallin (Fig. 6E).

The palps arise from the anterior-most ectoderm, which exhibits discrete and complementary patterns of *Islet*, *Btd* and *Emx* expression

(e.g. Fig. 1C'', C''', D''). Ultrastructural and neuroanatomical studies have reported three distinct cell types in the *Ciona* palps, although there are probably at least four (Dolcemascolo et al., 2009; Imai and Meinertzhagen, 2007). The interpapillary area marked by *Btd* might contain the adhesive-secreting cells, as the corresponding region in a related ascidian, *Botryllus schlosseri*, consists of secretory cells (Caicci et al., 2010). Small, round neurons called basal cells have been observed at the base of the papillae in *Ciona*; these basal cells might correspond to the *Emx*⁺ rings that delimit the protrusions (Imai and Meinertzhagen, 2007). Within the palp protrusions, there appear to be two distinct cell types. Spindle-shaped neurons (called anchor cells) with axons projecting into the brain are well-documented and believed to have a sensory function (Dolcemascolo et al., 2009; Imai and Meinertzhagen, 2007; Torrence and Cloney, 1983). The *Islet*⁺ cells we have described are marked by apical digitiform protrusions (Fig. 2G'), similar to the axial columnar cells previously reported (Dolcemascolo et al., 2009). We have never observed axons extending from these cells, and their function remains uncertain. It is possible that the *Islet*-expressing cells are secondary sensory cells that are innervated by trunk epidermal or other neurons.

It is noteworthy that in *Ciona*, *Islet* is expressed in additional cell types with unique and characteristic shapes: the otolith, the notochord and the A10.57 motoneuron (Giuliano et al., 1998; Stolfi and Levine, 2011). The otolith is a gravity-sensing pigmented cell with a highly polarized shape – an extension that protrudes from the cell body is elaborated into a broad 'foot' that inserts into the membrane of the sensory vesicle (Sakurai et al., 2004). The notochord cells, by contrast, are arranged as a flattened 'stack of coins' at the early tailbud stage. Later, as the tailbud matures, the notochord cells undergo a dramatic cell shape change, becoming elongated and cylindrical, followed by vacuolation and tubulogenesis (Denker and Jiang, 2012). The motor ganglion controls the swimming behavior of the tadpole and consists of five

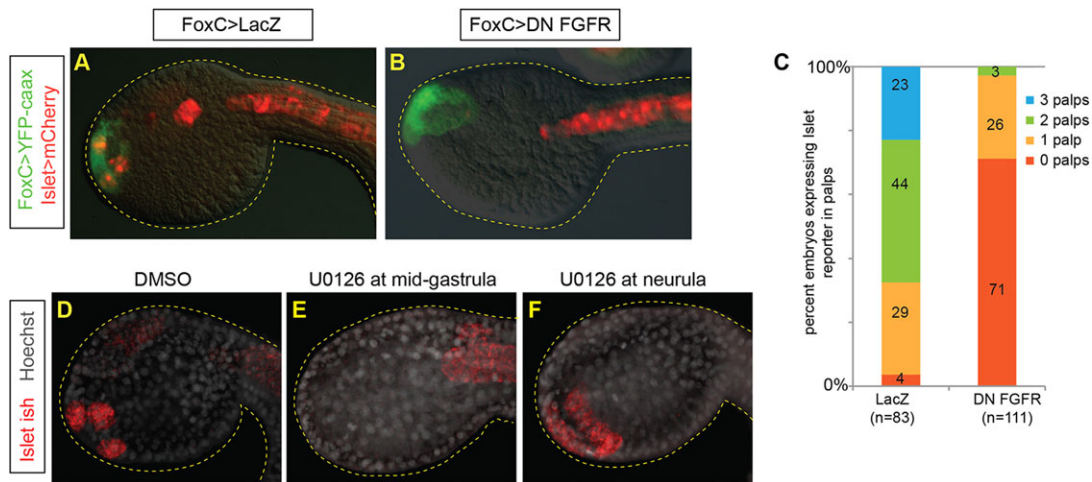


Fig. 5. Establishment of *Islet* pattern requires FGF-MAPK signaling through neurula stage. (A,B) *Islet>mCherry* reporter was co-expressed with *FoxC>YFP-caax* and either *FoxC>lacZ* (A) or *FoxC>DN FGFR* (B). Embryos were scored for *Islet* reporter expression at mid-tailbud stage, quantification shown in C. (D-F) *Islet* ISH of mid-tailbud stage embryos. Embryos were treated with U0126 at mid-gastrula stage (E) or at the early- to mid-neurula stage (F), and compared with control embryos incubated with DMSO (D). Nuclei are stained with Hoechst 33342.

pairs of neurons. Only the posterior-most pair, A10.57, expresses *Islet*, and its cell body is markedly elongated in comparison to the other motoneurons that do not express *Islet* (Stolfi and Levine, 2011). The identification of *Islet* target genes in the palps, notochord and otolith could reveal important cellular effector genes contributing to their distinctive elongated morphologies.

Islet belongs to a subclass of homeodomain transcription factors (together with *Lhx* and *Lmx*) distinguished by the presence of two LIM domains in the N-terminus. The LIM domain is a type of zinc finger that functions as a protein-binding platform with diverse functions (Kadmas and Beckerle, 2004; Zheng and Zhao, 2007). LIM-HD proteins require the nuclear cofactor *LIM-domain-binding protein-1* (*Ldb-1*, also known as *NLI* or *CLIM*) for activity (Matthews and Visvader, 2003). *Ldb-1* has a LIM-interaction domain (LID) that directly interacts with the LIM domains of *Islet*, as well as a dimerization domain, which enables the formation of complex multimeric protein assemblies that can activate or repress transcription (Jurata and Gill, 1997; Jurata et al., 1998). Expression

of isolated protein domains (either the *Ldb-1* LID, or the LIM domains from *Islet*) produces a dominant-negative phenotype by disrupting the native *Ldb-1-Islet* complexes. This approach produces cellular phenotypes similar to those obtained by DNA- and RNA-based loss-of-function assays (Becker et al., 2002; Segawa et al., 2001). The LIM domains are thus essential for the biological function of *Islet*. LIM domains are also found in a variety of proteins that associate with the actin cytoskeleton, many of which, although primarily cytosolic, have been shown to shuttle into and out of the nucleus. An emerging hypothesis is that LIM domains act as biosensors, communicating across cellular compartments to coordinate nuclear regulatory states with cytoskeletal activity (Kadmas and Beckerle, 2004). LIM-HD transcription factors may thus be uniquely well-suited for the genetic control of cell morphology.

Islet is expressed in a wide variety of neurons across metazoans (Jackman et al., 2000; Nomaksteinsky et al., 2013; Simmons et al., 2012; Voutev et al., 2009). Though widely known for its role in

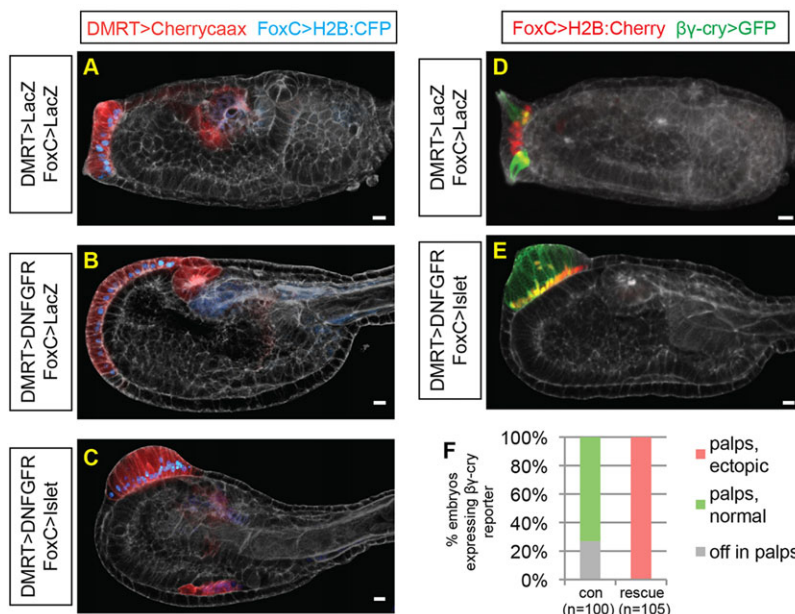


Fig. 6. *Islet* expression rescues palp development downstream of perturbed FGF-MAPK signaling.

(A-C) Larvae electroporated with *DMRT>Cherry-caax* and *FoxC>H2B:CFP* to label anterior neural plate and palp lineage, respectively. (A) Control larva expressing *DMRT>lacZ* and *FoxC>lacZ* shows normal palp development. (B) Expression of *DMRT>DN FGFR* leads to loss of palps, concomitant with ectopic *FoxC* expression that develops at the expense of the anterior sensory vesicle. (C) Expression of *DMRT>DN FGFR* and *FoxC>Islet* leads to formation of one large, protrusive palp. (D,E) Larvae expressing *FoxC>H2B:mCherry* and palp differentiation marker *beta-crystallin>GFP*. Control larva in D shows *beta-crystallin* reporter in two of the three palps but not in the intervening palp domain marked by *FoxC* reporter. (E) The single giant palp in larva expressing *DMRT>DN FGFR* plus *FoxC>Islet* shows ectopic expression of *beta-crystallin* reporter, concomitant with the *FoxC* expression domain. (F) Quantification of results shown in D,E. Scale bars: 10 μ m.

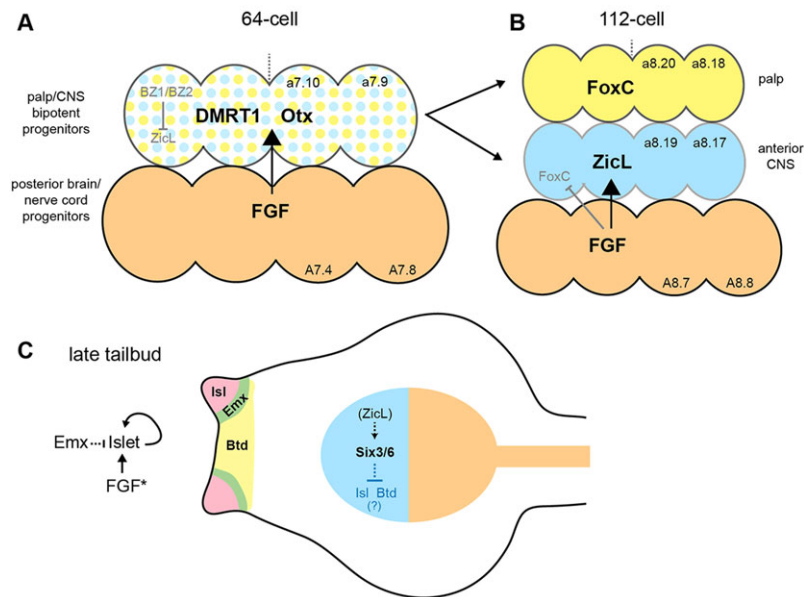


Fig. 7. Summary of gene regulatory network underlying palp development. Based on results of current and previous studies (Ikeda et al., 2013; Imai et al., 2006; Wagner and Levine, 2012). Genes in bold black font are expressed in indicated region; gray font indicates genes repressed in those areas; blue font denotes untested regulatory interactions; parentheses indicate genes that were expressed in progenitors of that region but have since been downregulated. (A,B) A subset of the neural progenitors at indicated stages. Dotted vertical line denotes midline. Blastomere names (according to ascidian nomenclature) indicated on right side. Lowercase and uppercase letters (e.g. a7. and A7.) refer to cells of animal and vegetal hemispheres, respectively. (A) At 64-cell stage, the bipotent palp/CNS progenitors express *DMRT1* and *Otx* in response to FGF signal from vegetal neural precursors. Bipotency requires active repression of *ZicL* by *BZ1/BZ2*. (B) At 112-cell stage, the palp and anterior CNS fates have segregated. Anterior CNS fate requires FGF signaling to induce *ZicL* and restrict *FoxC* to the palp lineage. (C) In late tailbud embryos, *Six3/6* is expressed in anterior brain, downstream of *ZicL*. (We speculate that *Islet* and *Btd* might be actively repressed in the anterior brain by *Six3/6*. This is because ectopic expression of *ZicL* in palp progenitors leads to repression of *Islet* and *Btd*, and this effect might be mediated by the *Six3/6* repressor.) The palps are the anterior-most region of specialized ectoderm (derived from *FoxC*⁺ population shown in B) expressing *Btd* and *Emx*, as well as the protrusions expressing *Islet*. *Emx* might function to limit *Islet* to discrete foci. *Islet* is expressed in response to FGF signaling (but see Fig. 5F) and is maintained by positive autoregulation.

motor neuron specification, it also functions in motor axon outgrowth in both *Drosophila* and vertebrates (Liang et al., 2011; Segawa et al., 2001; Thaler et al., 2004; Thor and Thomas, 1997). *Islet* orthologs are widely expressed in sensory neurons as well, where they also influence cell shape. Mouse *Isl2*, for example, is expressed in a subset of retinal ganglion cells that possess a distinctive morphology, with characteristic dendritic lamination patterns and axonal projection targets (Triplett et al., 2014). In zebrafish embryos, inhibition of *Isl2* results in aberrant axon positioning, as well as defective axon outgrowth and branching of Rohon–Beard and trigeminal sensory neurons (Andersen et al., 2011; Segawa et al., 2001). Similar defects have been reported upon inhibition of *Isl1* in both mouse and zebrafish (Liang et al., 2011; Tanaka et al., 2011). Neuron-specific *Islet* target genes have begun to be identified, and they are important for neural morphology (Aoki et al., 2014). Slit-mediated axon branching, for example, relies on *Isl2* target genes such as *PlexinA4* (Miyashita et al., 2004; Yeo et al., 2004). The *Islet*-dependent outgrowth and branching of axons and dendrites seen in vertebrates might have evolved from a simpler, ancestral regulatory network controlling cell shape, such as that featured in *Ciona*.

In summary, we have provided evidence that *Islet* functions downstream of FGF signaling to regulate target genes required for palp morphogenesis, including cellular effectors underlying elongation. Given the correlation between *Islet* expression and cell shape in both *Ciona* and vertebrates, it is conceivable that a detailed understanding of *Islet* function may help to illuminate mechanisms by which transcriptional regulation directs the process of cellular morphogenesis.

MATERIALS AND METHODS

Cell sorting and expression profiling

Cells of the specified palp lineage were isolated from dissociated embryos expressing the cell surface marker CD4:GFP using antibody-coupled magnetic beads. RNA was isolated from these isolated cells and hybridized to Affymetrix GeneChip microarray. See Methods in the supplementary material for details.

Molecular cloning

Cloning of *Islet*- and *DN FGFR*-coding sequences, and of enhancers for *DMRT*, *FoxC*, *FoxF*, *ZicL* and *β-crystallin*, has been described (Beh et al., 2007; Shimeld et al., 2005; Stolfi and Levine, 2011; Wagner and Levine, 2012). *Emx*-coding sequence (gene model KHL142.14.v1.A.ND1-1) was PCR-amplified from mixed stage cDNA with the oligos *Emx* cds NF: TAATGCGCCGCAACCATGATTCTTAACCAATCCCAC and *Emx* cds BlpR: TAATGCTCAGCTTACGTCATAGACGCTTGCGTTAC, and cloned into a plasmid downstream of the *FoxC* enhancer by standard methods. The DNA-binding domain of *Emx* was amplified with the oligos *Emx* DBD NheF: TAATGCTAGCTTATTGATGGCGAATCCATTTC and *Emx* DBD SpeR: TAATACTAGTGCTACCTTTCTCTTCGATTTC, and cloned upstream of the WRPW repression domain as described (Stolfi et al., 2011). *Islet* cis-regulatory DNA was pieced together from a 500 bp promoter region and the partial sequence of the first intron cloned upstream. The *Islet* promoter was amplified with *Isl* pro XhoF: TAATCTCGAGTTAACTTAACATGGGCGTGTG and *Isl* pro NR: TAATGCGCCGCTTCGTTGATAAACTTGTGAAC. The *Islet* intronic enhancer was amplified with *Islet* int1a AscF: TAATGGCGCGCCCTCGCTTAATTGCGGTAAG and *Islet* int1a XhR: TAATCTCGAGGCCAAACAAAACCTTTATTTTATTTTC. See supplementary material Fig. S1 for the complete sequence. The *Islet* DNA-binding domain was amplified with *Isl* DBD NheF: TAATGCTAGCTAAAGATGCGAAGACGACGCGAG and DBD NgoMIV R: TAATGCGGCCTTCGCTTGCTGCTCTCGATTTC, and cloned upstream of the

WRPW repressor motif to create Isl:WRPW. For details of molecular cloning of CD4:GFP and CD8:mCherry constructs see Methods in the supplementary material.

Embryo manipulation

Adult *Ciona intestinalis* animals were obtained from M-REP. Protocols for fertilization, dechoriation and electroporation have been described (Christiaen et al., 2009a,b). Plasmid concentration for electroporation varied between 40 and 80 µg per replicate; all experiments were performed at least twice. U0126 (Promega) was resuspended in DMSO and diluted to 10 µM in filtered artificial seawater (FASW). Phalloidin (Molecular Probes) was diluted 1:500 in PBT (PBS+0.1% Tween 20) and incubated with embryos overnight. Hoechst 33342 (Life Technologies) staining was performed at 2 µg/ml in PBT for 2–4 h. Imaging was performed on a Zeiss 700 laser scanning confocal microscope or Zeiss AxioImager.A2 upright microscope.

In situ hybridization (ISH)

DNA templates for *Islet*, *Six1/2* and *Btd* probe synthesis were obtained from *Ciona* Gene Collection Release 1 (clone numbers GC01d01, GC05e01 and GC02k02, respectively). The *Emx* probe was transcribed from the antisense strand of the coding sequence. The probe synthesis (Wagner and Levine, 2012) and double ISH protocol have been described (Stolfi et al., 2011). Briefly, antisense RNA probes were transcribed in the presence of either fluorescein-UTP (Roche) or digoxigenin-UTP (Roche). Probes were detected with peroxidase-conjugated antibodies (anti-DIG-POD, Roche 11207733910, 1:1000; or anti-Fluorescein-POD, Roche 11426346910, 1:1000) combined with tyramide signal amplification (Cy3 TSA kit or Fluorescein TSA kit, PerkinElmer). When present, GFP was detected with primary antibody rabbit anti-GFP (Invitrogen A-11122, 1:1000) and secondary antibody donkey anti-rabbit Alexa Fluor 488 (Invitrogen A-21206, 1:1000).

Cell length analysis

Confocal microscopy was used to image a total of 20 mosaic embryos each for the control (*FoxF>lacZ*) and the experiment (*FoxF>Islet*). A single section from each embryo was chosen for analysis. We chose sections in which the surface ectoderm of both the control and perturbed halves were clearly visible and free of distortions. A total of ten measurements were taken by hand with ImageJ software on each side (electroporated and unelectroporated), from similar positions along the anterior-posterior axis. The average measured length was used to generate the normalized value (electroporated/unelectroporated) for each embryo. We sought to avoid making measurements very near the palps, which are thickened, and near the trunk-tail junction, because sometimes this region appears pinched or distorted due to variation in the shape/orientation of embryos. *P*-values were calculated using the Wilcoxon two-sample test.

Acknowledgements

We thank Peter Walentek and Remi Dumollard for helpful discussion regarding cell length measurements, Wei Zhang for help with the box plot, Weiyang Shi for CD4:GFP and CD8:mCherry constructs and helpful discussion regarding magnetic cell sorting, and Emma Farley and Levine lab members for constructive feedback.

Competing interests

The authors declare no competing financial interests.

Author contributions

E.W. designed and performed the experiments and wrote the manuscript in consultation with A.S. and M.L. A.S. cloned *Islet* enhancer and *Islet*-coding sequences (full length and WRPW fusion). Y.G.C. prepared and analyzed microarray samples.

Funding

This work was supported by a National Science Foundation Postdoctoral Research Fellowship in Biology [NSF-1161835] to A.S. and by the National Institutes of Health (NIH) [NS076542]. Deposited in PMC for release after 12 months.

Supplementary material

Supplementary material available online at <http://dev.biologists.org/lookup/suppl/doi:10.1242/dev.110684/-/DC1>

References

- Andersen, E. F., Asuri, N. S. and Halloran, M. C. (2011). In vivo imaging of cell behaviors and F-actin reveals LIM-HD transcription factor regulation of peripheral versus central sensory axon development. *Neural Dev.* **6**, 27.
- Aoki, M., Segawa, H., Naito, M. and Okamoto, H. (2014). Identification of possible downstream genes required for the extension of peripheral axons in primary sensory neurons. *Biochem. Biophys. Res. Commun.* **445**, 357–362.
- Becker, T., Ostendorff, H. P., Bossenz, M., Schlüter, A., Becker, C. G., Peirano, R. I. and Bach, I. (2002). Multiple functions of LIM domain-binding CLIM/NLI/Ldb cofactors during zebrafish development. *Mech. Dev.* **117**, 75–85.
- Beh, J., Shi, W., Levine, M., Davidson, B. and Christiaen, L. (2007). FoxF is essential for FGF-induced migration of heart progenitor cells in the ascidian *Ciona intestinalis*. *Development* **134**, 3297–3305.
- Caicci, F., Zaniolo, G., Burighel, P., Degasperi, V., Gasparini, F. and Manni, L. (2010). Differentiation of papillae and rostral sensory neurons in the larva of the ascidian *Botryllus schlosseri* (Tunicata). *J. Comp. Neurol.* **518**, 547–566.
- Caracciolo, A., Di Gregorio, A., Aniello, F., Di Lauro, R. and Branno, M. (2000). Identification and developmental expression of three Distal-less homeobox containing genes in the ascidian *Ciona intestinalis*. *Mech. Dev.* **99**, 173–176.
- Christiaen, L., Wagner, E., Shi, W. and Levine, M. (2009a). Electroporation of transgenic DNAs in the sea squirt *Ciona*. *Cold Spring Harb. Protoc.* **2009**, pdb prot5345.
- Christiaen, L., Wagner, E., Shi, W. and Levine, M. (2009b). Isolation of sea squirt (*Ciona*) gametes, fertilization, dechoriation, and development. *Cold Spring Harb. Protoc.* **2009**, pdb prot5344.
- Delsuc, F., Brinkmann, H., Chourrout, D. and Philippe, H. (2006). Tunicates and not cephalochordates are the closest living relatives of vertebrates. *Nature* **439**, 965–968.
- Denker, E. and Jiang, D. (2012). *Ciona intestinalis* notochord as a new model to investigate the cellular and molecular mechanisms of tubulogenesis. *Semin. Cell Dev. Biol.* **23**, 308–319.
- Dolcemascolo, G., Pennati, R., De Bernardi, F., Damiani, F. and Gianguzzo, M. (2009). Ultrastructural comparative analysis on the adhesive papillae of the swimming larvae of three ascidian species. *Invert. Surviv. J.* **6**, S77–S86.
- Gans, C. and Northcutt, R. G. (1983). Neural crest and the origin of vertebrates: a new head. *Science* **220**, 268–273.
- Giuliano, P., Marino, R., Pinto, M. R. and De Santis, R. (1998). Identification and developmental expression of Ci-is1, a homologue of vertebrate islet genes, in the ascidian *Ciona intestinalis*. *Mech. Dev.* **78**, 199–202.
- Groppelli, S., Pennati, R., Scari, G., Sotgia, C. and De Bernardi, F. (2003). Observations on the settlement of *Phallusia mammillata* larvae: effects of different lithological substrata. *Ital. J. Zool.* **70**, 321–326.
- Hudson, C., Darras, S., Caillol, D., Yasuo, H. and Lemaire, P. (2003). A conserved role for the MEK signalling pathway in neural tissue specification and posteriorisation in the invertebrate chordate, the ascidian *Ciona intestinalis*. *Development* **130**, 147–159.
- Ikeda, T., Matsuoka, T. and Satou, Y. (2013). A time delay gene circuit is required for palp formation in the ascidian embryo. *Development* **140**, 4703–4708.
- Imai, J. H. and Meinertzhagen, I. A. (2007). Neurons of the ascidian larval nervous system in *Ciona intestinalis*: II. Peripheral nervous system. *J. Comp. Neurol.* **501**, 335–352.
- Imai, K. S., Hino, K., Yagi, K., Satoh, N. and Satou, Y. (2004). Gene expression profiles of transcription factors and signaling molecules in the ascidian embryo: towards a comprehensive understanding of gene networks. *Development* **131**, 4047–4058.
- Imai, K. S., Levine, M., Satoh, N. and Satou, Y. (2006). Regulatory blueprint for a chordate embryo. *Science* **312**, 1183–1187.
- Jackman, W. R., Langeland, J. A. and Kimmel, C. B. (2000). islet reveals segmentation in the *Amphioxus* hindbrain homolog. *Dev. Biol.* **220**, 16–26.
- Jurata, L. W. and Gill, G. N. (1997). Functional analysis of the nuclear LIM domain interactor NLI. *Mol. Cell. Biol.* **17**, 5688–5698.
- Jurata, L. W., Pfaff, S. L. and Gill, G. N. (1998). The nuclear LIM domain interactor NLI mediates homo- and heterodimerization of LIM domain transcription factors. *J. Biol. Chem.* **273**, 3152–3157.
- Kadmas, J. L. and Beckerle, M. C. (2004). The LIM domain: from the cytoskeleton to the nucleus. *Nat. Rev. Mol. Cell Biol.* **5**, 920–931.
- Liang, X., Song, M.-R., Xu, Z., Lanuza, G. M., Liu, Y., Zhuang, T., Chen, Y., Pfaff, S. L., Evans, S. M. and Sun, Y. (2011). Isl1 is required for multiple aspects of motor neuron development. *Mol. Cell. Neurosci.* **47**, 215–222.
- Manni, L., Lane, N. J., Joly, J.-S., Gasparini, F., Tiozzo, S., Caicci, F., Zaniolo, G. and Burighel, P. (2004). Neurogenic and non-neurogenic placodes in ascidians. *J. Exp. Zool. B Mol. Dev. Evol.* **302B**, 483–504.
- Matthews, J. M. and Visvader, J. E. (2003). LIM-domain-binding protein 1: a multifunctional cofactor that interacts with diverse proteins. *EMBO Rep.* **4**, 1132–1137.

- Mazet, F., Hutt, J. A., Milloz, J., Millard, J., Graham, A. and Shimeld, S. M. (2005). Molecular evidence from *Ciona intestinalis* for the evolutionary origin of vertebrate sensory placodes. *Dev. Biol.* **282**, 494-508.
- Miyashita, T., Yeo, S.-Y., Hirate, Y., Segawa, H., Wada, H., Little, M. H., Yamada, T., Takahashi, N. and Okamoto, H. (2004). PlexinA4 is necessary as a downstream target of Islet2 to mediate Slit signaling for promotion of sensory axon branching. *Development* **131**, 3705-3715.
- Nakayama-Ishimura, A., Chambon, J.-P., Horie, T., Satoh, N. and Sasakura, Y. (2009). Delineating metamorphic pathways in the ascidian *Ciona intestinalis*. *Dev. Biol.* **326**, 357-367.
- Nomaksteinsky, M., Kassabov, S., Chettouh, Z., Stoeklé, H.-C., Bonnaud, L., Fortin, G., Kandel, E. R. and Brunet, J.-F. (2013). Ancient origin of somatic and visceral neurons. *BMC Biol.* **11**, 53.
- Park, B. Y. and Saint-Jeannet, J. P. (2010). Molecular identity of cranial placodes. In *Induction and Segregation of the Vertebrate Cranial Placodes* (ed. D. S. Kessler), p. 20. San Rafael, CA: Morgan & Claypool Life Sciences.
- Pennati, R., Groppelli, S., De Bernardi, F., Mastroianni, F. and Zega, G. (2009). Immunohistochemical analysis of adhesive papillae of *Clavelina lepadiformis* (Müller, 1776) and *Clavelina plicifera* (Salfi, 1929) (Tunicata, Ascidiacea). *Eur. J. Histochem.* **53**, 25-34.
- Sakurai, D., Goda, M., Kohmura, Y., Horie, T., Iwamoto, H., Ohtsuki, H. and Tsuda, M. (2004). The role of pigment cells in the brain of ascidian larva. *J. Comp. Neurol.* **475**, 70-82.
- Sasakura, Y., Mita, K., Ogura, Y. and Horie, T. (2012). Ascidiaceans as excellent chordate models for studying the development of the nervous system during embryogenesis and metamorphosis. *Dev. Growth Differ.* **54**, 420-437.
- Schlosser, G. (2010). Making senses: development of vertebrate cranial placodes. *Int. Rev. Cell Mol. Biol.* **283**, 129-234.
- Segawa, H., Miyashita, T., Hirate, Y., Higashijima, S.-I., Chino, N., Uyemura, K., Kikuchi, Y. and Okamoto, H. (2001). Functional repression of Islet-2 by disruption of complex with Ldb impairs peripheral axonal outgrowth in embryonic zebrafish. *Neuron* **30**, 423-436.
- Shimeld, S. M., Purkiss, A. G., Dirks, R. P. H., Bateman, O. A., Slingsby, C. and Lubsen, N. H. (2005). Urochordate betagamma-crystallin and the evolutionary origin of the vertebrate eye lens. *Curr. Biol.* **15**, 1684-1689.
- Simmons, D. K., Pang, K. and Martindale, M. Q. (2012). Lim homeobox genes in the Ctenophore *Mnemiopsis leidyi*: the evolution of neural cell type specification. *EvoDevo* **3**, 2.
- Stolfi, A. and Levine, M. (2011). Neuronal subtype specification in the spinal cord of a protovertebrate. *Development* **138**, 995-1004.
- Stolfi, A., Gainous, T. B., Young, J. J., Mori, A., Levine, M. and Christiaen, L. (2010). Early chordate origins of the vertebrate second heart field. *Science* **329**, 565-568.
- Stolfi, A., Wagner, E., Taliaferro, J. M., Chou, S. and Levine, M. (2011). Neural tube patterning by Ephrin, FGF and Notch signaling relays. *Development* **138**, 5429-5439.
- Streit, A. (2008). The cranial sensory nervous system: specification of sensory progenitors and placodes. In *StemBook*, The Stem Cell Research Community: doi/10.3824/stembook.1.31.1.
- Svane, I. and Young, C. M. (1989). The ecology and behaviour of ascidian larvae. *Oceanogr. Marine Biol. Annu. Rev.* **27**, 45-90.
- Takamura, K. (1998). Nervous network in larvae of the ascidian *Ciona intestinalis*. *Dev. Genes Evol.* **208**, 1-8.
- Tanaka, H., Nojima, Y., Shoji, W., Sato, M., Nakayama, R., Ohshima, T. and Okamoto, H. (2011). Islet1 selectively promotes peripheral axon outgrowth in Rohon-Beard primary sensory neurons. *Dev. Dyn.* **240**, 9-22.
- Tassy, O., Dauga, D., Daian, F., Sobral, D., Robin, F., Khoeiry, P., Salgado, D., Fox, V., Caillol, D., Schiappa, R. et al. (2010). The ANISEED database: digital representation, formalization, and elucidation of a chordate developmental program. *Genome Res.* **20**, 1459-1468.
- Thaler, J. P., Koo, S. J., Kania, A., Lettieri, K., Andrews, S., Cox, C., Jessell, T. M. and Pfaff, S. L. (2004). A postmitotic role for Isl-class LIM homeodomain proteins in the assignment of visceral spinal motor neuron identity. *Neuron* **41**, 337-350.
- Thor, S. and Thomas, J. B. (1997). The *Drosophila* islet gene governs axon pathfinding and neurotransmitter identity. *Neuron* **18**, 397-409.
- Torrence, S. A. and Cloney, R. A. (1983). Ascidian larval nervous system: primary sensory neurons in adhesive papillae. *Zoomorphology (Berlin)* **102**, 111-123.
- Tresser, J., Chiba, S., Veeman, M., El-Nachef, D., Newman-Smith, E., Horie, T., Tsuda, M. and Smith, W. C. (2010). *doublesex/mab3 related-1 (dmrt1)* is essential for development of anterior neural plate derivatives in *Ciona*. *Development* **137**, 2197-2203.
- Triplet, J. W., Wei, W., Gonzalez, C., Sweeney, N. T., Huberman, A. D., Feller, M. B. and Feldheim, D. A. (2014). Dendritic and axonal targeting patterns of a genetically-specified class of retinal ganglion cells that participate in image-forming circuits. *Neural Dev.* **9**, 2.
- Voutev, R., Keating, R., Hubbard, E. J. A. and Vallier, L. G. (2009). Characterization of the *Caenorhabditis elegans* Islet LIM-homeodomain ortholog, *lim-7*. *FEBS Lett.* **583**, 456-464.
- Wagner, E. and Levine, M. (2012). FGF signaling establishes the anterior border of the *Ciona* neural tube. *Development* **139**, 2351-2359.
- Yeo, S.-Y., Miyashita, T., Fricke, C., Little, M. H., Yamada, T., Kuwada, J. Y., Huh, T.-L., Chien, C.-B. and Okamoto, H. (2004). Involvement of Islet-2 in the Slit signaling for axonal branching and defasciculation of the sensory neurons in embryonic zebrafish. *Mech. Dev.* **121**, 315-324.
- Zheng, Q. and Zhao, Y. (2007). The diverse biofunctions of LIM domain proteins: determined by subcellular localization and protein-protein interaction. *Biol. Cell* **99**, 489-502.